

Tracing rare earth elements in oil shale ash

Omar S. Al-Ayed^{(a)*}, Merania K. Qawaqneh^(b), Eyad S. M. Abu-Nameh^(b)

^(a) Department of Chemical Engineering, Faculty of Engineering Technology, Al-Balqa Applied University, Marka 11134, Amman, Jordan

^(b) Department of Chemistry, Faculty of Science, Al-Balqa Applied University, As-Salt 19117, Jordan

Received 14 February 2024, accepted 19 April 2024, available online 30 April 2024

Abstract. Oil shale ash generated from different locations in Jordan was investigated for rare earth elements (REE). The oil shale samples were combusted at 950 °C, and then milled to less than 74 µm. The resulting fine oil shale ash samples were acid-digested to remove minerals. The acid-digested residues were analyzed using inductively coupled plasma mass spectrometry. Fifteen REEs, along with yttrium and scandium, were detected, except for promethium. Among the detected metals, the highest concentrations were found for lanthanum and cerium, at 16.3 and 10.5 ppm, respectively, in the El-Lajjun deposits. The maximum concentration of REEs was 74.4 ppm in the Al-Shalaleh region, with a combined total of 47.06 ppm for light rare earth elements (LREE) and 29.31 ppm for heavy rare earth elements (HREE). The maximum calculated LREE/HREE ratio was 2.42 ppm in the Sultani region. The yttrium and scandium concentrations were 21.3 and 2.51 ppm in the El-Lajjun and Al-Shalaleh regions, respectively.

Keywords: rare earth elements, oil shale ash, ICP–MS, acid digestion.

1. Introduction

Oil shale is a sedimentary rock composed of two fractions: a hydrocarbon fraction containing kerogen, and a non-hydrocarbon fraction composed of inorganic metal and metal oxide components. When heated in the absence of air, the organic fraction produces shale oil, water, and light hydrocarbon gases in addition to hydrogen and carbon oxides. The solid product of retorted oil shale is referred to as spent shale. Upon oxidation or combustion to 900 °C, spent shale produces an inorganic fraction after the burning of fixed carbon and the decomposition of carbonates. Major inorganic constituents found in oil shale are quartz (SiO₂), feldspar (KAlSi₃O₈), apatite (Ca₅(PO₄)₃(F,Cl,OH)),

* Corresponding author, omar.alayed@bau.edu.jo

calcite (CaCO_3), pyrite (FeS_2), and dolomite ($\text{CaMg}(\text{CO}_3)$) [1].

Upon calcination of spent shale to produce oil shale ash, it was found to contain several metals and metal oxides [2]. On the other hand, analysis of oil shale ash [3] was found to contain, in addition to usual oxides and metal oxides, small amounts of REEs. The increasing demand for REEs in high-technology industries, such as electronics, makes these elements a limited strategic resource for development. In this regard, the presence of REEs in oil shale ash and coal ash, which are considered waste products of power plants, is worth investigating. The extraction of these elements would offer an alternative solution to address the scarcity of available deposits.

The X-ray fluorescence (XRF) and inductively coupled plasma mass spectrometry (ICP-MS) analyses of oil shale ash samples [3–10] have indicated the presence of various metal oxides, non-metals, and REEs. Coal ash was investigated for the presence of REEs, using microwave digestion and ICP-MS. The analysis of oil shale ash after microwave acid digestion, using ICP-MS, showed the presence of other non-metallic elements in minor amounts.

The presence of REEs in oil shale was investigated in 13 out of 28 samples (micritic limestone, marl, and oil shale) from the Shengli River–Changshe Mountain oil shale zone in China [3]. This study traced 15 elements in oil shale ash, with cesium exhibiting the highest concentrations ranging from 19.7 to 28.6 ppm, followed by lanthanum with values from 10 to 14.2 ppm, and yttrium with 8.7–10.7 ppm. On the contrary, the LREE/HREE ratio fluctuated between 7.1 and 8.5.

Birdwell [11] studied REEs in the Eocene Green River Formation, reporting the presence of all REEs and LREE/HREE ratios ranging from 0.8 to 355.5, depending on sample locations. Furthermore, the oil shale of the Yan'an Formation in the Tanshan area in China was investigated for REEs [12]. Results showed lanthanum concentrations ranging from 25.9 to 43.6 ppm, and cesium concentrations varying between 47.8 and 73.9 ppm, depending on the depth of studied samples. The reported LREE/HREE ratio was also found to depend on sample depth, ranging from 8.1 to 11.9 ppm.

Authors have tried to correlate REEs with the type of ore present in the oil shale. A detailed study of the heavy metal and trace element content of kukersite oil shale ash was conducted, using ICP-MS [13]. The relationship between REEs and other major elements in oil shale are found to be of terrigenous origin [9, 14, 15], controlled by wrack rather than by organic matter. The presence of REEs in Huadian oil shale has been presumed to show some correlative indications to the types of minerals present in the oil shale [14]. The presence of REEs is associated with monazite ($(\text{Ce,La,Nd,Th})\text{PO}_4 \cdot \text{SiO}_2$) [16]. This study reported that LREEs have a stronger occurrence with the sulfide mineral fraction, whereas HREEs were bound to other minerals, such as aluminosilicate, carbonate, and ferromanganese oxyhydroxides. In another study [10] on the Barren Measures Formation of the Jharia Basin, the total

concentrations of LREEs and HREEs were 200.1–305.1 and 22.3–32.8 ppm, respectively. These authors recommended the extraction of HREEs rather than LREEs due to the sample's richness in HREEs. For the enrichment of trace REEs from waste oil shale ash, the best experimental conditions are optimum temperature, acidity, reaction time, and solid/liquid ratio [17].

Recently, REEs in oil shale ash have received attention due to their stable geochemical characteristics and potential economic value. The distribution of REEs in oil shale ash has been widely used to characterize the source compositions of detrital sediments. However, very few studies have investigated the distribution of REEs in cretaceous oil shale [18]. REEs are important in advanced technology applications, and studies have shown that oil shale can be rich in REE content. Since Jordan oil shale reserves are huge and accessible for surface mining, it is worth exploring the economic viability of such elements. REEs include 17 elements. Among them, 15 are known as lanthanides, while yttrium (Y) and scandium (Sc) are also considered REEs. Yttrium and scandium tend to occur in the same ore deposits as lanthanides and exhibit similar chemical properties [19].

REEs are divided into two types (Table 1). The light REE group includes lanthanum (La), cerium (Ce), praseodymium (Pr), neodymium (Nd), promethium (Pm), samarium (Sm), europium (Eu), and gadolinium (Gd). The heavy REE group contains terbium (Tb), dysprosium (Dy), holmium (Ho), erbium (Er), thulium (Tm), ytterbium (Yb), and lutetium (Lu). REE metals are of silver or gray color, and with a notable luster, although they get easily oxidized in the air.

Table 1. Light and heavy rare earth elements

Lanthanides	LREEs	La	Ce	Pr	Nd	Pm	Sm	Eu	Gd
	HREEs	Tb	Dy	Ho	Er	Tm	Yb	Lu	

In Jordan, limited research has been conducted on the presence of REEs in different locations. Khoury [20] focused on analyzing bituminous marl, travertine, altered marble, veins, and cavity-filling sites in central Jordan, with an emphasis on travertine with secondary supergene minerals, using inductively coupled plasma optical emission spectrometry (ICP–OES). The study locations were situated near the El-Lajjun, Sultani, and Attarat oil shale deposits. The distribution of REEs was explored by Abdulkader and Murry [21], in the economic grade Jordanian Upper Cretaceous phosphorites (near Sultani and El-Lajjun oil shale deposits), who found that REEs showed a depletion in Ce and LREEs, in contrast to enrichment in HREEs, indicating marine depositional environment. Regarding REEs in Jordanian oil shale, Khoury [20] explored the presence of REEs in various oil shale ash samples.

2. Materials and methods

2.1. Oil shale

The oil shale samples were collected from different locations/deposits in Jordan, including Attarat Umm Al-Ghudran, El-Lajjun, Sultani, Jurf Al-Drawaish, Assfar Al-Mahata, Wadi Abu-Hmam, and Al-Shalaleh. The samples were crushed by a jaw crusher and screened using the British Sieving System (BSS). The particle diameters ranging between 8 and 20 mm (to achieve complete roasting and to avoid high pressure drop) were selected and burned in the oven at a temperature of 450–500 °C for four hours to oxidize hydrocarbons. This was followed by roasting (heating with hot air) in an electric furnace to a temperature above 950 °C to ensure the decomposition of dolomites and carbonates into oxides and carbon dioxide. The oil shale ash samples were milled using a ball mill and sieved to a size below 74 µm.

2.2. XRF analysis

An XRF spectrometer (S8 TIGER, Bruker AXS GmbH) was employed for the analysis of the micro components of oil shale ash. Samples from five selected regions were studied.

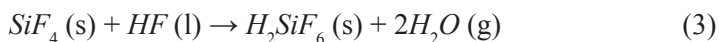
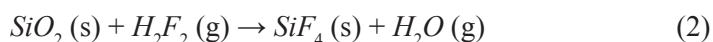
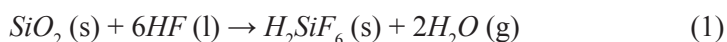
2.3. Acid digestion

2.3.1. Open cup digestion

A one-gram sample of milled oil shale ash, with a particle size less than 74 µm, was treated with a 30 mL mixture of acids. The mixture consisted of 15 mL of hydrofluoric acid, HF (48% purity), 10 mL of perchloric acid, HClO₄ (70% purity), and 5 mL of hydrochloric acid, HCl (35–38% purity). The ash sample and the mixed acids were placed together into a Teflon cup. The mixture was mixed and placed over a heater for four-five hours at 150–180 °C to digest minerals. This digestion process, outlined in Method 3050B (www.epa.gov), resulted in a precipitate containing REEs. The precipitated sludge was then washed with distilled water and filtered to remove contaminants or impurities before the final analysis. REEs in the filtrate were quantified, using various analytical equipment, such as ICP–MS and ICP–OES. During the digestion process, the most assumed reactions, as reported in the literature [22], were the following:

A. Hydrofluoric acid

i. Quartz removal:

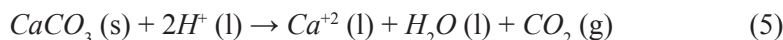


- ii. Silicate removal:

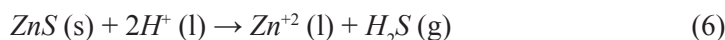


- B. Hydrochloric acid

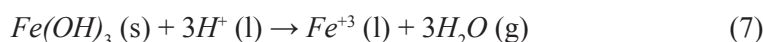
- i. Dissolution of carbonates:



- ii. Dissolution of zinc sulfides:



- iii. Dissolution of basic or amphoteric oxides and hydroxides:



2.3.2. Microwave digestion (closed cup)

A 0.1-gram sample of solid oil shale ash was dissolved in 5 mL of concentrated nitric acid, HNO_3 , in a microwave oven (in special closed Teflon cylindrical vessels). Each run was heated to 200 °C for 20 min, and kept at 200 °C and 16 bar pressure for another 25 min. The samples were then cooled for a minimum of 45 min to a temperature lower than 50 °C and opened for analysis. After microwave digestion, the content was cooled and diluted to 50 mL.

2.4. ICP–MS analysis

ICP–MS offers fast, multielement detection of elements at concentrations as low as the part per billion (ppb) range. However, scientists often face challenges in the measurement of REEs, including the occurrence of polyatomic and isobaric interferences that are not resolved by quadrupole ICP–MS. To address these challenges, the samples were analyzed using iCAP Q, a triple quadrupole ICP–MS 8800. The instrument parameters were plasma gas flow (14 L/min), auxiliary gas flow (0.8 L/min), argon carrier gas (0.8 L/min), collision/reaction cell gas setting (1.2 mL/min He), plasma RF power (1550 W), dwell time per mass (0.01–0.015 s), and scan speed (20 $\mu\text{m/s}$).

3. Results and discussion

3.1. XRF analysis

The analysis results indicated that silica (SiO_2) was the most abundant compound in oil shale ash, with its mass constituting between 30–50 wt%. Calcium oxide (CaO) followed as the second largest compound, with its mass ranging between 38–48 wt%. Other major oxides, such as Al_2O_3 , Fe_2O_3 , P_2O_5 , Na_2O , MgO , K_2O , TiO_2 and CrO_3 , were also detected but to a lesser degree. Some of the results are presented in Figure 1.

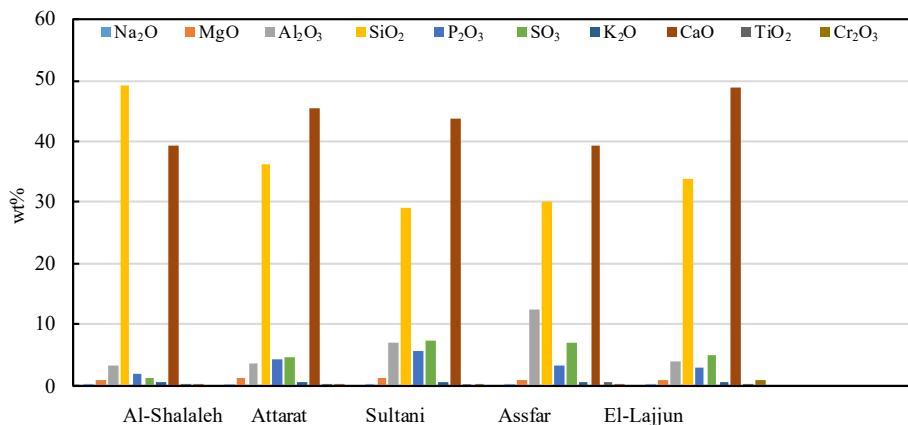


Fig. 1. Most abundant metal oxides in oil shale ash in different regions.

Similar results have been reported by several authors from Jordan [2, 23, 24]. The mass percentages of different reported oxides may vary, depending on the method of sample preparation, sample location, and the equipment employed for analysis.

3.2. REE analysis

Non-REEs present in different locations in Jordan, as detected by ICP–MS, are summarized in Table 2. The mass percentages of calcium, magnesium and iron are 39.7%, 2.8% and 1.4%, respectively, which makes them the most abundant elements in oil shale ash.

Based on Table 2, calcium is the predominant element, with its mass percentages fluctuating between 34% and 39% of the sample weight depending on the region. Silicon is the second most abundant element, with its mass percentage ranging from 13.4% to 18%. Other metals, such as Mg, Fe and Al, are available in lower percentages.

Table 3 shows REEs in oil shale ash, detected and quantified by ICP–MS. All REEs were present in all locations of the study, except for Pm, which either was not present or fell below the detection limit of the equipment. As seen from the table, among the different REEs, La is the most abundant element, with approximately 16 and 27 ppm in El-Lajjun and Al-Shalaleh, respectively. Ce is the second most abundant element, with around 10 and 15 ppm in El-Lajjun and Al-Shalaleh, respectively. These two elements are LREEs.

The total sum of LREEs (Σ LREE) ranges between 6.02 and 91.3 ppm, depending on the region, whereas the total sum of HREEs (Σ HREE) is much lower than that of LREEs, i.e., 2.7 and 57.01 ppm, respectively. Meanwhile, the total sum of REEs (Σ REE) ranged from 8.7 ppm for Attarat to 148.31 ppm for Al-Shalaleh, and the LREE/HREE ratio varied according to the region.

Table 2. Non-REEs present in oil shale ash in different regions, ppm

Element	Attarat Umm Al-Ghudran	Sultani	El-Lajjun	Assfar Al- Mahata	Al- Shalaleh	Wadi Abu- Hmam	Jurf Al- Drawaish
Li +/- mg/kg	0.79 0.01	7.95 0.14	15.63 0.25	6.44 0.05	15.40 0.18	3.99 0.09	0.56 0.01
Be +/- mg/kg	0.06 0.01	0.39 0.01	0.43 0.01	0.22 0.02	0.42 0.01	0.20 0.00	0.11 0.01
Na +/- mg/kg	140.37 3.23	239.36 2.39	387.39 2.32	264.49 1.85	406.18 2.84	246.17 0.25	212.24 2.33
Mg +/- mg/kg	2824.33 8.47	3883.49 93.20	3672.54 14.69	3202.85 41.64	3631.75 58.11	3185.21 47.78	1374.24 26.11
Al +/- mg/kg	787.85 21.27	7387.17 162.52	7969.52 151.42	3277.23 52.44	7847.14 141.25	3975.25 27.83	2403.77 31.25
Si +/- mg/kg	179660.11 2265.27	136565.0 142.52	161244.3 851.42	142026.8 952.44	228981.7 1141.25	133975.25 127.83	162403.77 31.25
P +/- mg/kg	156.71 2.51	1854.54 22.25	3470.38 72.88	1757.08 82.58	3487.92 55.81	1781.38 62.35	680.39 12.93
S +/- mg/kg	310.18 59.87	314.46 62.89	3596.76 136.68	2777.46 49.99	4101.15 139.44	373.50 73.58	<LOD <LOD
K +/- mg/kg	207.26 1.24	2113.84 12.68	3079.40 27.71	1309.38 89.04	3050.43 39.66	1381.24 34.53	257.70 2.32
Ca +/- mg/kg	397455.57 4769.47	369432 482.62	338376.11 2368.63	399589.58 32766.35	347610.50 9733.09	397006.6 11513.19	395108.0 5136.40
Ti +/- mg/kg	20.60 0.12	180.20 0.6	176.04 0.70	73.63 0.59	196.08 1.18	105.77 1.16	33.21 0.66
V +/- mg/kg	35.45 0.78	82.31 1.07	16178 3.56	51.05 1.23	187.43 5.25	46.60 2.00	50.41 0.96
Cr +/- mg/kg	10.90 0.17	90.12 0.72	163.76 3.28	64.94 1.88	160.72 3.5	51.69 2.17	35.01 0.53
Mn +/- mg/kg	28.15 0.34	52.72 0.26	74.57 1.04	39.62 0.24	91.21 1.46	35.65 0.07	1924.57 25.02
Fe +/- mg/kg	1428.13 8.57	6866.58 48.07	9943.86 119.33	4808.54 177.92	9750.32 126.75	4548.59 177.40	1025.27 7.18
Co +/- mg/kg	0.23 0.00	1.19 0.01	1.52 0.01	0.59 0.01	1.40 0.01	0.39 0.00	1.16 0.02
Ni +/- mg/kg	7.20 0.07	22.60 0.16	70.57 0.56	31.84 0.16	73.05 0.29	15.06 0.24	13.47 0.08
Cu +/- mg/kg	3.30 0.05	7.65 0.11	28.09 0.20	11.97 0.05	27.98 0.25	3.96 0.05	3.82 0.07

<LOD – below the limit of detection

For example, the lowest ratio was recorded in Jurf Al-Drawaish, at 1.43, and the highest in Sultani, at 2.42. The presence of LREEs exceeds the availability of HREEs in all studied samples, which aligns with the findings of Khoury [20]. However, this is in contradiction with the findings of Bai et al. [14], who reported the association of LREEs with the sulfide mineral fraction, while HREEs were bound to other minerals, such as aluminosilicate, carbonate, and ferromanganese oxyhydroxides, since Jordanian oil shales are rich in aluminosilicate and dolomite.

Table 3. REEs present in oil shale ash in different regions, ppm

Element	Attarat Umm Al-Ghudran	Sultani	El-Lajjun	Assfar Al-Mahata	Al-Shalaleh	Wadi Abu-Hmam	Jurf Al-Drawaish
La	1.55	6.61	16.3	8.31	27.4	4.55	6.58
Ce	1.8	8.73	10.5	4.92	15.7	5.73	3.69
Pr	0.3	1.25	2.7	1.29	3.8	0.8	0.92
Nd	1.26	4.87	10.9	5.22	40.3	3.32	3.95
Pm	n.d.	n.d.	n.d.	n.d.	n.d.	n.d.	n.d.
Sm	0.25	0.91	2.1	0.95	4.1	0.62	0.71
Eu	0.6	0.21	0.5	0.24	0.6	0.15	0.18
Gd	0.26	0.89	2.4	1.15	2.9	0.64	0.87
Tb	0.04	0.12	0.3	0.16	0.6	0.09	0.12
Dy	0.23	0.75	0.12	1.06	2.0	0.6	0.77
Ho	0.05	0.2	0.47	0.23	0.6	0.1	0.2
Er	0.14	0.4	1.4	0.72	2.2	0.3	0.5
Tm	0.02	0.06	0.2	0.1	2.6	0.05	0.07
Yb	0.12	0.35	1.2	0.65	2.7	0.3	0.4
Lu	0.02	0.05	0.2	0.11	0.6	0.04	0.1
Y	1.8	6.13	21.3	11.02	39.7	4.95	9.2
Sc	0.28	1.65	2.6	1.21	2.51	1.13	0.48
Σ REE	8.72	33.18	73.19	37.34	148.31	23.37	28.74
Σ LREE	6.02	23.47	45.4	22.08	91.3	15.81	16.9
Σ HREE	2.7	9.71	27.79	15.26	57.01	7.56	11.84
$(\Sigma$ LREE / Σ HREE) ratio	2.23	2.42	1.63	1.45	1.60	2.09	1.43

n.d. – not determined

Figure 2 shows the presence of LREEs in different locations. As seen from the figure, La is the most abundant element, with concentrations ranging from 1.6 to 16 ppm. Among LREEs, La, Ce and Nd exhibit higher concentrations compared to other elements, while the presence of Eu, Gd and Sm is minimal.

Figure 3 presents the concentrations of HREEs. As seen from the figure, Dy in the Sultani region is available in a small concentration lower than 2.5 ppm. The concentrations of Lu, Tm and Ho are below 0.5 ppm. In general, all HREEs exhibit very low concentrations, which limits the prospects of commercial mining.

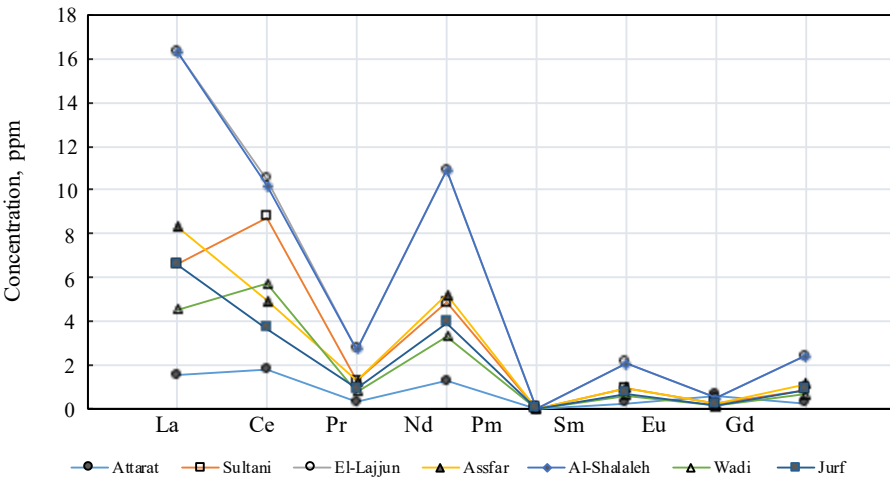


Fig. 2. LREEs and their concentrations in different locations.

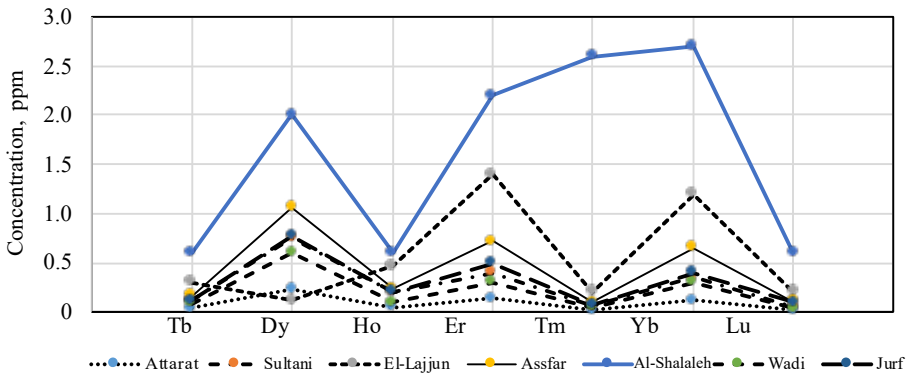


Fig. 3. HREEs and their concentrations in different locations.

4. Conclusions

Oil shale ash samples from seven locations were investigated for rare earth elements. Fifteen REEs, along with yttrium and scandium, were detected, except for promethium, which was below the detection limit. The total sum of REEs present in the samples ranged between 8.7 and 74.37 ppm, depending on the region. The low concentrations of REEs in Jordanian oil shale ash do not encourage commercial utilization. Among light REEs, lanthanum and cerium were found to be the most abundant elements. The presence of heavy REEs was observed to be much lower than that of LREEs. The maximum concentration of all REEs was 74.4 ppm, which is considered insignificant compared to other available research.

Acknowledgments

This study was supported by the Deanship of Scientific Research & Innovation, Al-Balqa Applied University (grant No. DSR-2021#387). The publication costs of this article were covered by the Estonian Academy of Sciences.

REFERENCES

1. Shanks, W. C., Seyfried, W. E., Meyer, W. G., O'Neil, T. J. Mineralogy of oil shale. *Developments in Petroleum Science*, 1976, **5**, 81–102.
2. Al-Thunibat, I. M., Al-Harabsheh, A., Aljbour, S. H., Shawabkeh, A. Chemical and mechanical properties of Attarat (Jordan) oil shale ash and its engineering viable options. *Solid Fuel Chemistry*, 2023, **57**(2), 138–146.
3. Fu, X., Wang, J., Zeng, Y., Tan, F., He, J. Geochemistry and origin of rare earth elements (REEs) in the Shengli River oil shale, northern Tibet, China. *Geochemistry*, 2011, **71**(1), 21–30.
4. Al-Harabsheh, M., Al-Ayed, O., Robinson, J., Kingman, S., Al-Harabsheh, A., Tarawneh, K., Saeid, A., Barranco, R. Effect of demineralization and heating rate on the pyrolysis kinetics of Jordanian oil shales. *Fuel Processing Technology*, 2011, **92**(9), 1805–1811.
5. Qing, W., Jingru, B., Jianxin, G., Yan-Zhen, W., Shuyuan, L. Geochemistry of rare earth and other trace elements in Chinese oil shale. *Oil Shale*, 2014, **31**(3), 266–277.
6. Kaljuvee, T., Trass, O., Pihu, T., Konist, A., Kuusik, R. Activation and reactivity of Estonian oil shale cyclone ash towards SO₂ binding. *Journal of Thermal Analysis and Calorimetry*, 2015, **121**, 19–28.
7. Thompson, R. L., Bank, T., Montross, S., Roth, E., Howard, B., Verba, C., Granite, E. Analysis of rare earth elements in coal fly ash using laser ablation inductively coupled plasma mass spectrometry and scanning electron microscopy.

- Spectrochimica Acta Part B: Atomic Spectroscopy*, 2018, **143**, 1–11.
8. Park, S., Kim, M., Lim, Y., Yu, J., Chen, S., Woo, S. W., Yoon, S., Bae, S., Kim, H. S. Characterization of rare earth elements present in coal ash by sequential extraction. *Journal of Hazardous Materials*, 2021, **402**, 123760.
 9. Bai, Y., Liu, Z., Sun, P., Liu, R., Hu, X., Zhao, H., Xu, Y. Rare earth and major element geochemistry of Eocene fine-grained sediments in oil shale- and coal-bearing layers of the Meihe Basin, northeast China. *Journal of Asian Earth Sciences*, 2015, **97**(A), 89–101.
 10. Tiwari, B., Ghosh, S., Kumar, S., Varma, A. K. Trace and rare earth elements in the Permian shales: geochemical paradigms. *Arabian Journal of Geosciences*, 2023, **16**(4), 272–294.
 11. Birdwell, J. E. *Review of Rare Earth Element Concentrations in Oil Shales of the Eocene Green River Formation*. Open-File Report 2012–1016. U.S. Geological Survey, Reston, 2012.
 12. Hai, L., Xu, Q., Mu, C., Tao, R., Wang, L., Bai, J., Song, Y. Geochemical characteristics and geologic significance of rare earth elements in oil shale of the Yan'an Formation in the Tanshan area, in the Liupanshan Basin, China. *Interpretation*, 2021, **9**(3), T843–T854.
 13. Konist, A., Neshumayev, D., Baird, Z. S., Anthony, E. J., Maasikmets, M., Järviok, O. Mineral and heavy metal composition of oil shale ash from oxyfuel combustion. *ACS Omega*, **5**(50), 2020, 32498–32506.
 14. Bai, J. R., Wang, Q., Wei, Y. Z., Liu, T. Geochemical occurrences of rare earth elements in oil shale from Huadian. *Journal of Fuel Chemistry and Technology*, 2011, **39**(7), 489–494.
 15. Bai, Y., Lv, Q., Liu, Z., Sun, P., Xu, Y., Meng, J., Meng, Q., Xie, W., Wang, J., Wang, K. Major, trace and rare earth element geochemistry of coal and oil shale in the Yuqia area, Middle Jurassic Shimengou Formation, northern Qaidam Basin. *Oil Shale*, 2020, **37**(1), 1–31.
 16. Behring, T., Deacon, G. B., Junk, P. C. The chemistry of rare earth metals, compounds, and corrosion inhibitors. In *Rare Earth-Based Corrosion Inhibitors* (Forsyth, M., Hinton, B., eds). Woodhead Publishing, 2014.
 17. Yang, H., Wang, W., Zhang, D., Deng, Y., Cui, H., Chen, J., Li, D. Recovery of trace rare earths from high-level Fe³⁺ and Al³⁺ waste of oil shale ash (Fe–Al–OSA). *Industrial & Engineering Chemistry Research*, 2010, **49**(22), 11645–11651.
 18. Hu, F., Meng, Q., Liu, Z., Xu, C., Zhang, X. Petrology, mineralogy, and geochemical characterization of Paleogene oil shales of the Youganwo Formation in the Maoming Basin, southern China: implication for source rock evaluation, provenance, paleoweathering and maturity. *Energies*, 2023, **16**(1), 514.
 19. Balaram, V. Rare earth elements: a review of applications, occurrence, exploration, analysis, recycling, and environmental impact. *Geoscience Frontiers*, 2019, **10**(4), 1285–1303.
 20. Khoury, H. N. Industrial rocks and minerals of Jordan: a review. *Arabian Journal of Geosciences*, 2019, **12**(20), 619–658.

21. Abed, A. M., Murry, O. S. A. Rare earth element geochemistry of the Jordanian upper cretaceous phosphorites. *Arab Gulf Journal of Scientific Research*, 1997, **15**(1), 41–61.
22. Saxby, J. D. Isolation of kerogen in sediments by chemical methods. *Chemical Geology*, 1970, **6**, 173–184.
23. Abu El-Rub, Z., Kujawa, J., Albarahmieh, E., Al-Rifai, N., Qaimari, F., Al-Gharabli, S. High throughput screening and characterization methods of Jordanian oil shale as a case study. *Energies*, 2019, **12**(16), 3148.
24. Gougazeh, M., Alsaqoor, S., Borowski, G., Alsafasfeh, A., Hdaib, D. I. The behavior of Jordanian oil shale during combustion process from the El-Lajjun deposit, central Jordan. *Journal of Ecological Engineering*, 2022, **23**(8), 133–140.